BULLETIN OF THE POLISH ACADEMY OF SCIENCES
TECHNICAL SCIENCES, Vol. 71(1), 2023, Article number: e143645
DOI: 10.24425/bpasts.2022.143645

A new closed-form formula for calculating a weakly singular static potential integral with linear current source distribution on a triangle

Anna GRYTSKO* and **Piotr SŁOBODZIAN**

Wrocław University of Science and Technology, Faculty of Information and Communication Technology, Wybrzeże Wyspiańskiego 27, 50-370 Wrocław, Poland

Abstract. The article presents a closed-form formula for solving a weakly singular surface integral with a linear current source distribution associated with the SIE-MoM formulation used for solving electromagnetic (EM) problems. The analytical formula was obtained by transforming the surface integral over a triangular domain into a double integral, and then directly determining formulas for the inner and outer integrals. The solution obtained is marked by high computational efficiency, high accuracy, and very simple implementation. The derived formula, in contrast to the currently available formulas, consists of quantities that have a clear and simple geometric interpretation, related to the geometry of the computational domain.

Key words: static vector potential integral, linear current source distribution, analytic integration, weakly singular integrals, isoparametric transformation, integration over a triangular domain.

1. INTRODUCTION

The analysis of EM fields on the surface of a scatterer (e.g. a conducting body) using the SIE-MoM approach (surface integral equation – method of moments) involves weakly singular surface integrals. Such integrals arise when the observed field is determined in the source region, i.e. when the observation point and the source point coincide ($|\vec{r}-\vec{r}'| \to 0$).

The problem of the appearance of a weakly singular kernel of the integral function appears not only in EM problems, but also in other fields of engineering, for example in microwave technique [1], avionics [2], in finding wave propagation and elasticity in acoustics [3], in problems of heat transfer and when describing wave distribution on the water surface, etc.

This paper uses as an example the evaluation of the so-called scattered fields (radiating fields) over a scatterer, describing a new analytical solution of weakly singular static potential integrals with a linearly varying current source distribution over a triangular domain. Most of the integration methods described in the literature are applied to the so-called reaction integrals, which involve integrating the subintegral function twice over the surface of the same triangle or two different triangles. In the case of the calculation of radiated fields, there is only one surface integral, which does not help solve the singularity problem at all.

Although many analytical and numerical methods for computing singular surface integrals over a triangular domain are known, much attention is still given to this problem. The mainstream of research is concerned with increasing the accuracy of computation while reducing the required computational complexity. In most practical applications (e.g. in CAD simulators), the so-called regular (non-singular) surface integrals are computed using various types of cubature and quadrature, with Gauss-Legendre quadratures being most commonly used [4–8]. This approach gives sufficiently accurate results when computing radiated fields far from a given EM field source distribution, i.e. in the far field. Unfortunately, the accuracy of Gauss-Legendre quadratures decreases dramatically when the observation point of the radiated field is close to the EM field source distribution or even when it lies in the EM field source region [7]. In this case, it is necessary to use special integration methods based on so-called adaptive cubature/quadrature or analytical integration methods.

There are several methods for obtaining an analytic representation of singular integrals over a triangular domain. Best-known methods include: the method of singularity subtraction [9–12]; the method of singularity cancellation [4–8, 13, 14]; the method of integration using power series [15]; and the method using integral theorems in vector analysis (e.g. the divergence theorem [9, 10] or Stokes' theorem [16]).

In the method of singularity subtraction, the singular part of the subintegral function is subtracted from this function and the separated singular integral (static part of the potential) is determined in closed form. The remaining integral (the dynamic part of the potential) is calculated numerically [8–10, 12]. For example, in [9, 10] it is shown that the analytical form of the singular integral can be determined using the divergence theorem, which allows for the transformation of the surface integral to a contour integral along the perimeter of a triangle.

*e-mail: anna.grytsko@pwr.edu.pl

Manuscript submitted 2022-06-13, revised 2022-09-22, initially accepted for publication 2022-10-22, published in January 2023.

In turn, in the method of singularity cancellation, the main accent is on the transformation to a local coordinate system such that the Jacobian of the transformation cancels the singularity [4, 7, 13, 14]. On the other hand, in [6] singularity cancellation was obtained by means of a special substitution with one of the integration variables, which made the subintegral function analytical in the integration domain. The authors used this fact to numerically compute the integral using Gauss-Legendre quadrature (they did not derive closed-form formulas). In contrast, paper [8] presents a method for regularization of a surface singular integral using generalized Duffy transformation to remove the singularity in the integrand. This idea has been extended in [13], and then in [7, 14], where an extension of the singularity removal scheme was proposed, consisting of a sequence of coordinate transformations of the integral domain (triangle) in combination with a change of the order of integration. Generally, the method of singularity cancellation has more advantages than the method of singularity subtraction [6].

The method of integration using series consists of the transformation of the subintegral function into a power series [15]. In this case, the form of the transformed subintegral function and the accuracy of calculations depend on the number of terms of the series included in the integral function expansion. The advantage of this method is the small number of integration domain transformations necessary to determine the coefficients used in the final analytical formula.

Finally, it is worth mentioning that analytical methods documented in the literature are not always simple to implement. For example, the method of transforming the surface integral to the contour integral using Stokes' theorem, described in [17], leads to numerous closed formulas. Unfortunately, the way they are derived is not clear, and the resulting relations are complicated and computationally intensive, even compared to numerical methods.

The main drawback of the above-mentioned integration methods stems from complicated computational domain transforming procedures, which lead to high computational complexity. Moreover, these methods have been developed mainly for calculating singular reaction integrals [7, 8, 13, 14, 17] rather than singular radiation integrals. To the authors' knowledge, there are no publications describing (in an accessible way) analytical formulas for calculating the singular integral for the static part of the magnetic vector potential generated by a linear time-harmonic current density distribution on a plane triangular surface. Generally, closed-form formulas are available in [4, 9, 10, 15, 16], however, their implementation is difficult without a clear understanding of the integration method being applied. In this paper, we propose a new analytical formula to calculate the singular integral for the static part of the magnetic vector potential generated by a linear current source density distribution over a triangle. The proposed formula is expressed in terms of quantities with a very simple geometric interpretation. Our formula is computationally more efficient than the formulas described in other works. The derivation of this formula is based on the removal of singularities by dividing the domain of integration into three smaller sub-domains [4, 7, 13, 14], and then applying a double transformation of the computational domain. First, a transformation from a global Cartesian coordinate system XYZ to the local rectangular coordinate system $UV\beta$ is effected, followed by transformation to the polar coordinate system $\rho\varphi$. We present a description of each transformation step, the derivation of the final analytical formulas, and their verification. In addition, we show the influence of the choice of the local coordinate system $UV\beta$ on the form of the final formula for calculating the singular integral. To ensure reproducibility of the results of our work and to provide comparative results, the proposed method has been compared with the state-of-the-art method described in [10].

2. FORMULATION OF THE PROBLEM

The scattered (radiated) field $\mathbf{E}^s$ on the surface of a 3-D object can be determined using the magnetic vector potential $\mathbf{A}$ induced by the time-harmonic current density distribution $\mathbf{J}_s$ on the surface of this object [18]. Current density distribution can be found, for example, by using the SIE-MoM approach, with a piece-wise linear approximation of $\mathbf{J}_s$ over triangular subdomains. The simplest form of this approximation is based on the so-called roof-top basis functions [19, 20]. A single vector roof-top basis function describes linear current source density distribution over pairs of adjacent triangular elements T_n^+ and T_n^-, as illustrated in Fig. 1. The function is defined as follows [19–22]:

$$\mathbf{B}_n\left(\bar{r}'\right) = \begin{cases} \dfrac{l_n}{2S_n^+} \cdot \bar{\rho}^+\left(\bar{r}'\right) & \bar{r}' \in T_n^+, \\ \dfrac{l_n}{2S_n^-} \cdot \bar{\rho}^-\left(\bar{r}'\right) & \bar{r}' \in T_n^-, \\ 0 & \text{otherwise}, \end{cases} \tag{1}$$

where l_n denotes the length of the common edge of the pair of triangles, $\bar{\rho}$ denotes the vector of position on the surface of the given triangle, S_n denotes the area of the given triangle, and $\bar{r}'$ is the position vector of the source point. In the following we will focus on determining the value of the surface integral only for the static part of the magnetic vector potential $\mathbf{A}$, generated by the linear distribution of the current density on the surface of the triangle T_n^+ (in the case of T_n^- we proceed identically).

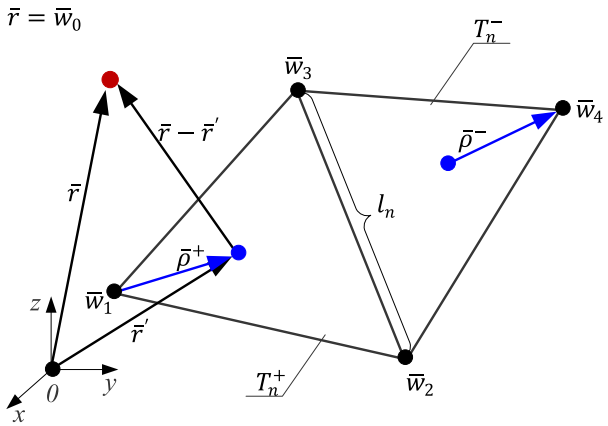

Fig. 1. The geometry of the current density distribution on T_n^+, T_n^-

After neglecting the scaling constants, the aforementioned integral takes the following form:

$$\mathbf{I}_0 = \iint\limits_{T_n^+} \frac{\overline{\rho}^+(\overline{r}')}{|\overline{r}-\overline{r}'|}\,\mathrm{d}S'. \tag{2}$$

3. THE PROPOSED METHOD

The proposed method is based on the cancellation of the singularity appearing at the vertex of the triangle that lies at the center of the coordinate system. In this case, the cancellation takes advantage of the Jacobian of the transformation of the integral from the rectangular coordinate system to the polar coordinate system, as shown in equation (3) (for T lying in the XY plane):

$$\begin{aligned}\mathbf{I} = \iint\limits_{T} \frac{f(\overline{r}')}{|\overline{r}'|}\,\mathrm{d}S' &= \int\limits_{\varphi_1}^{\varphi_2}\int\limits_{0}^{\rho_0(\varphi')} \frac{f(\rho')}{\cancel{\rho'}}\cancel{\rho'}\,\mathrm{d}\rho'\,\mathrm{d}\varphi' \\ &= \int\limits_{\varphi_1}^{\varphi_2}\int\limits_{0}^{\rho_0(\varphi')} f\left(\rho'\right)\mathrm{d}\rho'\,\mathrm{d}\varphi',\end{aligned} \tag{3}$$

where $\overline{r}'$ describes the position vector of the source point, $f(\overline{r}')$ denotes the current density distribution function, while the quantities appearing in the double integral on the right-hand side of the equation are described in Fig. 2.

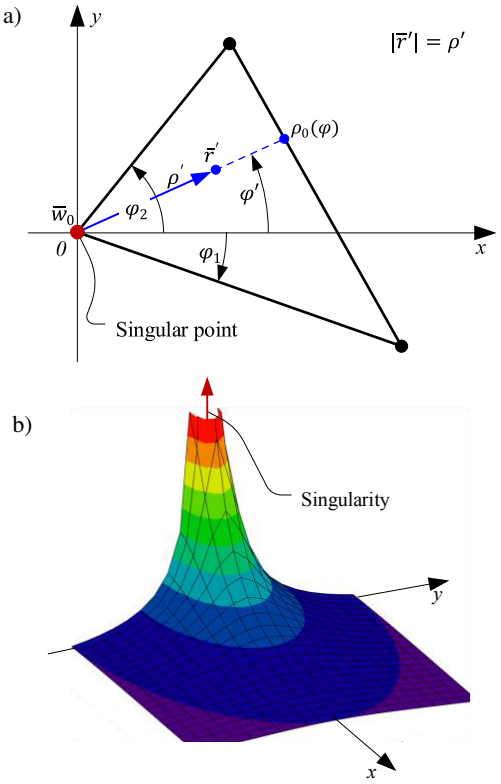

Fig. 2. Illustration of a triangle for singularity cancellation method in a subintegral function: a) the suitable triangle; b) the graph of an example of the integral function $f(\overline{r}')$ with singularity in the point $\overline{w}_0$. The position of the source point is defined relative to the center of the coordinate system. The singularity must be located at the vertex of the triangle, which is located at the center of the coordinate system

The case described in equation (3) can be generated artificially by transferring the surface integration to a new coordinate system, the center of which lies at the singular point $\overline{w}_0$ [4, 13]. Unfortunately, this approach requires controlling the limits of integration in polar coordinates and considering different cases, and the final formulas are in the form of complex trigonometric expressions [13].

Our method is based on the same technique (see also [4–7, 13, 14]), but its implementation is different from the one encountered so far, leading to simplified final formulas. The new method consists of four steps: (I) division of the domain of integration T_n^+ into three disjoint triangles T_1, T_2, and T_3 in such a way that the singular point $\overline{w}_0$ lies at a common vertex of these triangles, as shown in Fig. 3; (II) applying the isoparametric transformation [23] to move to a local coordinate system $UV\beta$, where the singular point $\overline{w}_0$ is located at the origin of the coordinate system (Fig. 4a); (III) transformation of the surface integral from the UV coordinate system to the polar coordinate system $\rho\varphi$ and then conversion of the surface integral into a double integral (Fig. 4b); (IV) determination of analytical formulas for the inner and outer integrals in the sequence.

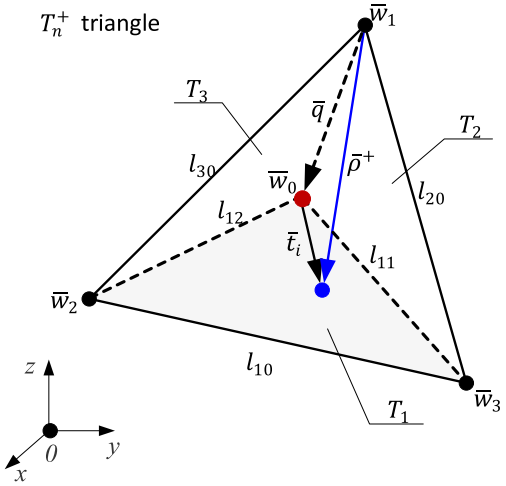

Fig. 3. Division of the domain of integration T_n^+ into subdomains T_1, T_2, and T_3

We shall apply the described steps to the case where the observation point $\overline{w}_0$ lies exactly in the area of the domain of integration T_n^+, i.e. on the surface of a triangle. According to the concept of singularity cancellation, in the first step, we divide the computational domain into three triangles T_1, T_2, and T_3 in such a way that $\overline{w}_0$ lies at the vertex of each of them (see Fig. 3). In this situation, equation (2) can be expressed as a sum of integrals calculated for consecutive triangles T_i ($i = 1, \ldots, 3$), namely:

$$\mathbf{I}_0 = \sum_{i=1}^{N=3} \mathbf{I}_{0i}, \tag{4}$$

where $\mathbf{I}_{0i}$ denotes the surface integral determined over T_i as in equation (2). The numbering of the side lengths for each i-th triangle starts from the outer side (l_{i0}) and then along successive sides counterclockwise, i.e. l_{i1} and l_{i2} (see, e.g. T_1 in Fig. 3).

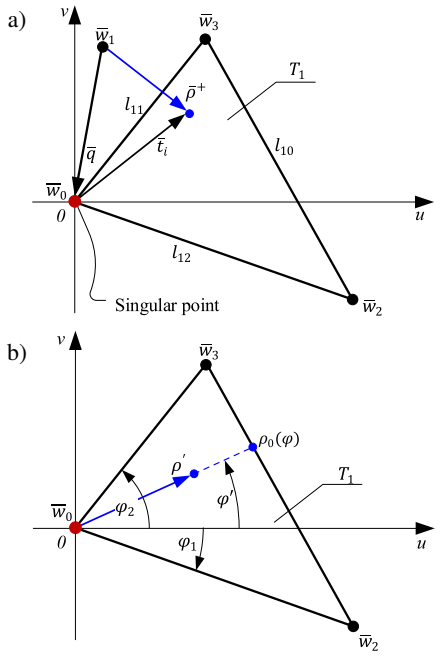

Fig. 4. Transformation of a triangle T_i (for $i = 1$): a) from the coordinate system XYZ to the local $UV\beta$ coordinate system; b) from the UV coordinate system to polar coordinate system $\rho\varphi$

In the second step, we transform triangle T_i (e.g. $i = 1$) to the local coordinate system $UV\beta$ [7, 10] or rather to the UV coordinate system, which spans the plane of triangle T_i. In this transformation, we assume that the basis vector $\bar{i}_{\beta i}$ is perpendicular to the plane of T_i and it is only needed to find the vector $\bar{i}_{vi}$. In the UV coordinate system the observation point $\overline{w}_0$ is the center of the coordinate system (see Fig. 4a). At this stage, we do not yet assume a particular form of the transformation $XYZ \to UV\beta$. We only assume that the vectors $\bar{r}$, $\bar{r}'$ and $\overline{\rho}^+(\bar{r}'$ are expressed in the UV system using local vectors $\bar{t}_i$ and $\overline{q}$, as shown in Fig. 3. In such a case, the integral $\mathbf{I}_{0i}$ takes the following form:

$$\mathbf{I}_{0i} = \iint_{T_i} \frac{\bar{t}_i + \overline{q}}{|\bar{t}_i|}\,\mathrm{d}A', \tag{5}$$

where $|\bar{t}_i| = |\bar{r} - \bar{r}'|$, wherein $\bar{t}_i = \bar{i}_{ui} \cdot u' + \bar{i}_{vi} \cdot v'$ is a vector defined in the UV coordinates (i.e. in the local coordinates of the triangle) by the following parametric equation with parameters u' and v':

$$|\bar{t}_i| = \sqrt{\left|\bar{i}_{ui}\right|^2 u'^2 + 2\left(\bar{i}_{ui} \cdot \bar{i}_{vi}\right) u'v' + \left|\bar{i}_{vi}\right|^2 v'^2}\,. \tag{6}$$

Vectors $\bar{i}_{ui}$ and $\bar{i}_{vi}$ are the basis vectors of the local UV coordinate system of the i-th triangle (they are defined in the XYZ coordinate system).

In the next step, we transform equation (5) from the local UV coordinate system to the polar coordinate system $\rho\varphi$ and then transform $\mathbf{I}_{0i}$ into a double integral [7]. Precisely, this step deletes the singularities of the subintegral function. Figure 4b shows the elements necessary to describe the limits of integration in the double integral. In order to perform the transformation, the variables in the UV coordinate system should be expressed using new variables of the polar coordinate system $\rho\varphi$, namely: $u' = \rho' \cdot \cos(\varphi')$, $v' = \rho' \cdot \sin(\varphi')$ and $\bar{t}_i = \rho' \cdot \cos(\varphi') \cdot \bar{i}_{ui} + \rho' \cdot \sin(\varphi') \cdot \bar{i}_{vi}$ The transition to the double integral in the polar coordinate system involves the Jacobian $J = \left|\bar{i}_{ui} \times \bar{i}_{vi}\right| \rho'\,\mathrm{d}\rho'\,\mathrm{d}\varphi'$. Accordingly, equation (5) transforms into equation (7) (see below), where $A_i = |\bar{i}_{ui}|^2$, $B_i = |\bar{i}_{vi}|^2$, $C_i = 2\left(\bar{i}_{ui} \cdot \bar{i}_{vi}\right)$ are constants, and the upper limit of the internal integral is $\rho_0(\varphi') = O_i/[\sin(\varphi') - L_i\cos(\varphi')]$, while L_i and O_i are coefficients of the equation of a line $v' = -L_i \cdot u' + O_i$ in the UV system, on which lies the side l_{i0} of triangle T_i.

$$\mathbf{I}_{0i} = \left|\bar{i}_{ui} \times \bar{i}_{vi}\right| \cdot \int_{\varphi_1}^{\varphi_2} \int_{0}^{\rho_0(\varphi')} \frac{\overline{q} + \left[\bar{i}_{ui}\cos(\varphi') + \bar{i}_{vi}\sin(\varphi')\right] \cdot \rho'}{\sqrt{A_i\cos^2(\varphi') + C_i\cos(\varphi')\sin(\varphi') + B_i\sin^2(\varphi')}}\,\mathrm{d}\rho'\,\mathrm{d}\varphi', \tag{7}$$

The choice of basis vectors of the isoparametric transformation is arbitrary (there are infinitely many possibilities). In our work, we discuss two cases. In Case I the basis vectors are defined in such a way that the original triangle T_i is transformed into a normalized triangle in the UV system, shown in Fig. 5a. In Case II the basis vectors are orthonormal, and their definition is taken from [10]. The triangle obtained in this case is shown in Fig. 5b. The first transformation introduces fixed integration limits to the double integral (regardless of the shape of the original triangle), while the second transformation requires determining the integration limits for each new triangle from scratch

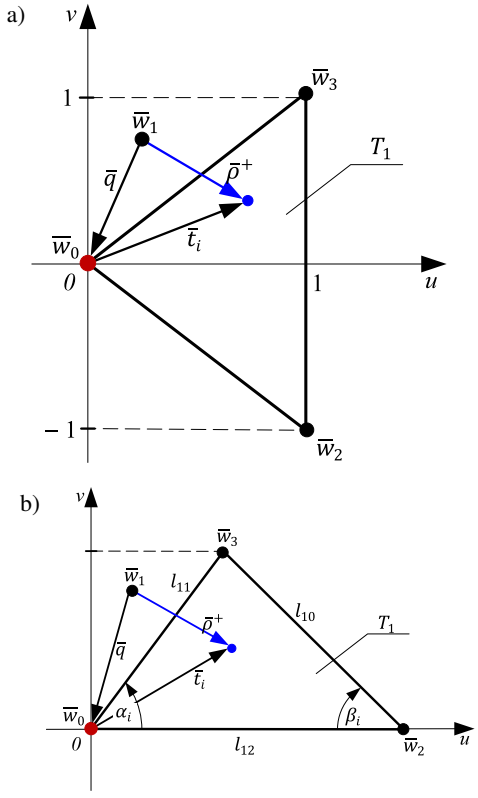

Fig. 5. Transformation of the triangle Ti (for $i = 1$) from the XYZ coordinate system to the local UV: a) Case I – normalized (scaled) triangle; b) Case II – a triangle with the original dimensions, with the side l_{12} along the axis u

(the limits are described by functions). The unit vectors $\bar{i}_{ui}$ and $\bar{i}_{vi}$ in Case I and Case II, respectively, are defined as follows (for $i = 1$):

$$\text{Case I} \qquad \bar{i}_{u1} = \frac{\overline{w}_3 - \overline{w}_2}{2} - \overline{w}_0\,, \qquad \bar{i}_{v1} = \frac{\overline{w}_3 - \overline{w}_2}{2}\,, \tag{8a}$$

$$\text{Case II} \qquad \bar{i}_{u1} = \frac{\overline{w}_2 - \overline{w}_0}{|\overline{w}_2 - \overline{w}_0|}\,, \qquad \bar{i}_{v1} = \bar{i}_{\beta 1} \times \bar{i}_{u1}\,. \tag{8b}$$

In both cases, the unit vector $\bar{i}_{\beta i}$ is normal to the surface T_i and can be determined by the vector product of the vectors defining the sides of the triangle T_i starting from vertex $\overline{w}_0$. In these cases, the unit vectors $\bar{i}_{ui}$ and $\bar{i}_{vi}$ (defined in the original coordinate system) have the properties (9a) and (9b). Equation (9a) describes the case illustrated in Fig. 5a, while equation (9b) describes the case in Fig. 5b. Taking into account the properties of the unit vectors, equation (7) takes the form of (10a) and (10b), for Case I and Case II, respectively, where the upper limit of inner integration in Case I is described by the relation $\rho_0(\varphi') = 1/\cos(\varphi')$, while in Case II by $\rho_0(\varphi') = O_i/[\sin(\varphi') - L_i\cos(\varphi')]$. For $i = 1$, we have $O_1 = L_1 w_{2x}$ and $L_1 = w_{3y}/(w_{2x} - w_{3x})$, where coordinates $\overline{w}_2$ and $\overline{w}_3$ are determined in the UV system.

$$\text{Case I} \qquad |\bar{i}_{ui}| \neq |\bar{i}_{vi}| \neq 1, \tag{9a}$$

$$\text{Case II} \qquad |\bar{i}_{ui}| = |\bar{i}_{vi}| = 1, \tag{9b}$$

Case I

$$\mathbf{I}_{0i} = S_i \cdot \int_{-\frac{\pi}{4}}^{\frac{\pi}{4}} \int_{0}^{\rho_0(\varphi')} \frac{\overline{q} + \left[\bar{i}_{ui}\cos(\varphi') + \bar{i}_{vi}\sin(\varphi')\right] \cdot \rho'}{\sqrt{A_i\cos^2(\varphi') + C_i\cos(\varphi')\sin(\varphi') + B_i\sin^2(\varphi')}}\,\mathrm{d}\rho'\mathrm{d}\varphi', \tag{10a}$$

Case II

$$\mathbf{I}_{0i} = \int_{0}^{a_i} \int_{0}^{\rho_0(\varphi')} \left(\overline{q} + \left[\bar{i}_{ui}\cos(\varphi') + \bar{i}_{vi}\sin(\varphi')\right] \cdot \rho'\right) \mathrm{d}\rho'\mathrm{d}\varphi'. \tag{10b}$$

The final step is to analytically solve formula (10a) and formula (10b) [24, 25]. After transformations and simplifications, these formulas take the form of equation (11a) and equation (11b), respectively.

Case I

$$\mathbf{I}_{0i} = \frac{S_i}{2\sqrt{B_i}} \cdot \left[\frac{\bar{i}_{vi}(l_{i1} - l_{i2})}{\sqrt{B_i}} + \frac{\bar{i}_{vi} C_i}{2B_i}\ln(D_i) + \left(\bar{i}_{ui} + 2\overline{q}\right)\ln(E_i)\right], \tag{11a}$$

Case II

$$\mathbf{I}_{0i} = \frac{J_i^2}{2}\left[J_i(Z_i\mathbf{F}_i - \mathbf{G}_i)\ln\left(\frac{X_i + Y_i(1 - J_i)}{X_i - Y_i(1 + J_i)}\right) + (\mathbf{F}_i + Z_i\mathbf{G}_i)\left(\frac{1}{Z_i H_i - K_i} - \frac{1}{Z_i}\right)\right]. \tag{11b}$$

In these formulas, the auxiliary variables are expressed by the following relationships:

$$A_i' = \sqrt{B_i}\, l_{i2}\,, \tag{12a}$$

$$A_i'' = \sqrt{B_i}\, l_{i1}\,, \tag{12b}$$

$$B_i' = A_i'' + C_i + B_i\,, \tag{12c}$$

$$B_i'' = A_i' + C_i - B_i\,, \tag{12d}$$

$$D_i = \frac{B_i''(A_i'' - C_i - B_i)}{B_i'(A_i' - C_i + B_i)}\,, \tag{12e}$$

$$E_i = \frac{B_i'}{B_i''}\,, \tag{12f}$$

$$\mathbf{F}_i = O_i^2\bar{i}_{ui} - 2O_i L_i\overline{q}, \tag{12g}$$

$$\mathbf{G}_i = O_i^2\bar{i}_{vi} + 2O_i\overline{q}, \tag{12h}$$

$$H_i = \frac{l_{i2}l_{i1} - 2(p_i - l_{i2})(p_i - l_{i1})}{l_{i2}l_{i1}} = \cos(\alpha_i)\,, \tag{12i}$$

$$J_i = \frac{l_{i2}l_{i0} - 2(p_i - l_{i2})(p_i - l_{i0})}{l_{i2}l_{i1}} = \cos(\beta_i)\,, \tag{12j}$$

$$K_i = 2S_i/l_{i2}l_{i1} = \sin(\alpha_i)\,, \tag{12k}$$

$$S_i = \sqrt{p_i(p_i - l_{i2})(p_i - l_{i0})(p_i - l_{i1})}\,, \tag{12l}$$

$$X_i = -2S_i/l_{i2}l_{i0} = -\sin(\beta_i)\,, \tag{12m}$$

$$Y_i = \sqrt{\frac{(p_i - l_{i2})(p_i - l_{i1})}{p_i(p_i - l_{i0})}} = \tan\left(\frac{\alpha_i}{2}\right), \tag{12n}$$

$$Z_i = -\frac{2S_i}{l_{i2}l_{i0} - 2(p_i - l_{i2})(p_i - l_{i0})} = -\tan(\beta_i)\,, \tag{12o}$$

where l_{i0}, l_{i1}, and l_{i2} are lengths of sides of triangle T_i, p_i is half the perimeter of the triangle and S_i is the area of the triangle.

Table 1 summarizes the quantities needed to calculate formula (11a) and formula (11b). All these quantities can be ex-

Table 1
Comparison of the geometric quantities needed for calculating equation (7) with M1, M2 and M3

No.	Quantities		
	M1	M2	M3
1	l_{i0}, l_{i1}, l_{i2}		
2	$\overline{q} = \overline{w}_0 - \overline{w}_1$		
3	$\bar{i}_{ui}$, $\bar{i}_{vi}$		
4	p_i, S_i		S_i
5	$\lvert\bar{i}_{vi}\rvert$, $\lvert\bar{i}_{vi}\rvert^2$	$\bar{i}_{\beta i}$	
6	$(\bar{i}_{ui} \cdot \bar{i}_{vi})$	–	
7	–	O_i, L_i	–
8	–		unit vectors $\parallel$ to l_{i0}, l_{i1}, l_{i2}
9	–		unit vectors $\perp$ to l_{i0}, l_{i1}, l_{i2}
10	–		distance btw. $\overline{w}_0$ and l_{i0}, l_{i1}, l_{i2}
11	–		distance btw. $\overline{w}_0$ and vertexes of T_i
12	–		derivatives and additional variables

pressed by position vectors of vertices of triangle T_i (e.g. for $i = 1$, we use $\overline{w}_0$, $\overline{w}_2$, and $\overline{w}_3$ defined in the XYZ coordinate system).

4. COMPUTATIONAL COMPLEXITY OF THE PROPOSED METHOD

To estimate the computational complexity of calculating integral $\mathbf{I}_{0i}$, the number of mathematical operations associated with formula (11a) (method M1), formula (11b) (method M2) and method of [10] (method M3) was estimated (see Table 2). The total computational complexity when calculating a single integral $\mathbf{I}_{0i}$ using M1, M2 and M3 is as follows:

$$\text{M1} \qquad N = O\left[n^2\left(2\sqrt{n}+19\right)\right], \tag{13a}$$

$$\text{M2} \qquad N = O\left[n^2\left(\sqrt{n}+41\right)\right], \tag{13b}$$

$$\text{M3} \qquad N = O\left[n^2\left(\sqrt{n}+50\right)\right], \tag{13c}$$

where N describes the total computational complexity, whereas n denotes the number of digits in the result of the calculation under assumed precision of computations.

Table 2
Comparison of the mathematic operations needed for calculating equation (7) with M1, M2 and M3

Operation	Computational complexity big O notation [26]	Number of operations		
		M1	M2	M3
$\log(x)$	$O(n^2\sqrt{n})$	2	1	1
$x \cdot y$	$O(n^2)$	12	27	27
x/y	$O\left(n^2\right)$	5	10	13
x^2	$O(n^2)$	1	2	7
$\sqrt{x}$	$O(n^2)$	1	1	3
Total computational complexity N for $n = 16$ digits:		6 912	11 520	12 800

It is worth adding that when calculating integral $\mathbf{I}_0$ in equation (2), the computational effort is $3 \times N$. In our case, the double precision of computations ($n = 16$) is used, and thus the computational complexity of M1 is ca. 1.6 times smaller than the computational complexity using M2, and ca. 2 times smaller than the computational complexity using M3.

The actual ratio of computational complexity may be different because the computational complexity of mathematical operations depends on their implementation in a given processor, and their execution time additionally depends on the operating system used.

To confirm the above results, a computational experiment was conducted to compare the computation speed using M1, M2 and M3. All computations were performed in a MATHCAD environment on a laptop computer (notebook) with an Intel(R) Core(TM) i7-9750H processor type, with clock frequency of 2.60 GHz and an MS Windows 10 operating system. As a result of the tests, it was found that computation time for $\mathbf{I}_{0i}$ using M1 is approx. 1.4 times faster than the computation time using M2 and approx. 2.2 times faster than the computation time using M3. The result obtained is close to the theoretical estimate. The lower computational complexity of M1 is mainly due to the lower amount of additional input data when compared to M2. The same can be said for the formulas derived in [10], where it is necessary to determine additional tangent and normal vectors to the sides of the triangle T_i.

The real computational gain for M1 can be estimated using an example of a specific computational task performed in the FEKO program, the well-known CAD tool in computational electromagnetics (CEM). As an example of the scattered field calculation ($\mathbf{E}^s$) by the SIE-MoM method, a perfectly conducted metal telecommunication container of the following dimensions: $10\lambda \times 8.13\lambda \times 9.41\lambda$ (i.e. $3.0 \times 2.4 \times 2.8$) was analyzed at the frequency of 1 GHz. When performing the calculations, the FEKO tool replaced the metal object with an appropriate calculation grid, which amounted to $n = 167218$ triangular elements. Now, let us assume that the calculation of $\mathbf{E}^s$ is done in 50 different points, located on the surface of the object. Let these points be located on the grid at the edge of adjacent triangles. This means that the number of weakly singular integrals for the calculations of $\mathbf{E}^s$ equals 100 (2×50), so equation (2) must be calculated 100 times.

In this case, the estimated time of computation of the weakly singular integral $\mathbf{I}_0$ for a single triangle using M1, M2 and M3 was 112.2 ms, 161 ms and 249.15 ms, respectively. In this situation the total time of computations of $\mathbf{E}^s$ in 50 points on the container under test would equal to 11.2 s, 16.1 s and 24.9 s, respectively. The computation time for M1 is 1.4 times faster than for M2 and ca. 2.2 times faster than for M3.

5. VALIDATION OF THE PROPOSED METHOD

Three different triangles were selected to validate methods M1, M2 and M3. The triangles were defined on the XY plane in order to simplify calculations in MATLAB and MATHCAD. The geometry of the triangles is shown in Fig. 6. The first triangle (a), having the worst quality factor, was chosen from [7]. The second one (b) was chosen arbitrarily. The last one (c), taken from [6], is poorly defined in terms of computations.

In the validation of the proposed formulas, reference values were calculated using equations described in [10] (they are widely accepted by the CEM community). For each of the methods, the average time needed to calculate equation (2) over one triangle was calculated. Additionally, internal procedures (based on adaptive quadratures) available in MATLAB and MATHCAD were also used. The validation results (see Tables 3–5) verify the excellent performance of M1 as compared to the other methods, including formulas in [10]. The results obtained using M1 and M2 and the method of [10] are identical for all the triangles that were put to the test. It is worth noting that there are still special points on the triangle at which not all methods produce a result (e.g. triangle (c) at point $\overline{w}_{02}$). In addition, M2 has a drawback in the case of $\beta = \pi/2$. For this case,

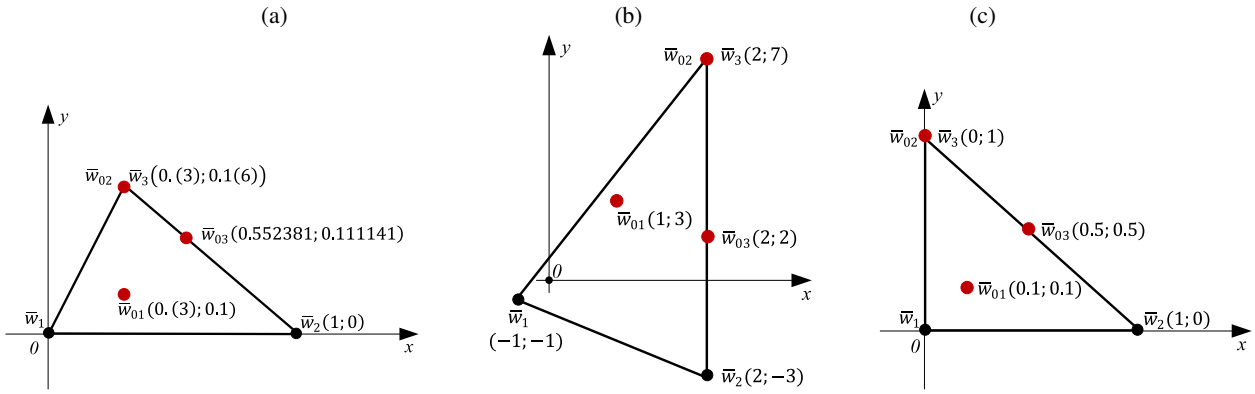

Fig. 6. The geometry of testing triangle with vertexes and testing (observation) points information

Table 3. Comparison of the results and the errors in calculating equation (2) with different methods for the triangle (a) in Fig. 6

No.	Method	Observation point/ computational time [ms]					
		$\overline{w}_{01}$	t_{01}	$\overline{w}_{02}$	t_{02}	$\overline{w}_{03}$	t_{03}
1.	M1	0.30670736486	112.2	0.22278374635	109.5	0.32541552401	113
2.	M2	0.30670736486	161.72	0.22278374635	164.3	0.32541552401	162.3
3.	M3	0.30670736486	249.15	–	255.12	0.32541552401	247.13
4.	MC	0.30670736485	987.15	0.22278374635	980.5	0.32541552400	984.4
5.	ML	0.30670736560	301	0.22278334194	300	0.32541675338	302.1
Error							
6.	|M1–M3|	0	_	–	_	0	_
7.	|M1–MC|	1.0E-11		1.0E-11		2.0E-12	
8.	|M1–ML|	7.4E-10		4.4E-7		1.2E-6	
9.	|MC–ML|	2.7E-10		1.3E-7		8.4E-6	

Abbreviations:

M1 – calculations using formula (11a)
M2 – calculations using formula (11b)
M3 – calculations using method of [10]
MC – calculations using MATHCAD
ML – calculations using MATLAB

Table 4. Comparison of the results and the errors in calculating equation (2) with different methods for the triangle (b) in Fig. 6

No.	Method	Observation point/ computational time [ms]					
		$\overline{w}_{01}$	t_{01}	$\overline{w}_{02}$	t_{02}	$\overline{w}_{03}$	t_{03}
1.	M1	21.6868908606	106.05	7.30886615859	107.15	20.2498538853	106
2.	M2	21.6868908606	155.55	7.30886615859	134.8	20.2498538853	157.17
3.	M3	21.6868908606	256.65	7.30886615859	257.2	20.2498538853	253.31
4.	MC	21.6868970507	300.2	7.30886614861	290.5	20.2499062820	295.02
5.	ML	21.6865432312	227.05	7.30886622709	216.5	20.2498540221	220
Error							
6.	|M1–M3|	0	_	0	_	0	_
7.	|M1–MC|	6.2E-6		1.0E-8		5.2E-5	
8.	|M1–ML|	3.4E-4		6.9E-8		1.4E-7	
9.	|MC–ML|	2.7E-10		1.3E-7		8.4E-6	

Table 5
Comparison of the results and the errors in calculating equation (2) with different methods for the triangle (c) in Fig. 6

No.	Method	Observation point/ computational time [ms]					
		$\overline{w}_{01}$	t_{01}	$\overline{w}_{02}$	t_{02}	$\overline{w}_{03}$	t_{03}
1.	M1	0.45039298059	112.1	0.20710678118	110.1	0.66103019026	111.23
2.	M2	0.45039298059	145.65	–	142.35	0.66103019026	145
3.	M3	0.45039298059	251.03	–	259.33	0.66103019026	252.43
4.	MC	0.45039298059	599	0.20710678118	597.8	0.66103019026	600.2
5.	ML	0.45039567842	280	0.20715678216	282	0.66103896578	281.3
Error							
6.	|M1–M3|	0	–	–	–	0	–
7.	|M1–MC|	0		0		0	
8.	|M1–ML|	2.7E-6		5.0E-5		8.8E-6	
9.	|MC–ML|	2.0E-6		4.0E-6		8.0E-6	

the (11b) analytical formula does not give the correct answer because it diverges. The absolute error calculated between our formula, i.e. equation (11a), and the referenced one in [10] is zero and depends only on the level of precision of the processor. In turn, the differences in results obtained using our formula and adaptive quadratures in MATLAB and MATHCAD are quite considerable. It is worth noting that results produced by MATLAB and MATHCAD differ quite considerably, too (see line 6 Table 5), however MATHCAD's procedure for adaptive integration still seems more accurate than the MATLAB's one.

6. CONCLUSIONS

In this paper, we proposed analytical formula (11a) (method M1) for calculating the weakly singular integral of the static vector potential with linearly varying current source distribution on the triangular surface. We confirmed the correctness of the computer implementation of the derived formula and its higher computational efficiency. The proposed formula is simple, making it possible to obtain high accuracy of calculations with less computational complexity in comparison with formula (11b) and the state-of-the-art formulas described in [10].

The quantities used in formula (11a) have a simple geometric interpretation, which facilitates correct implementation of the formula.

REFERENCES

[1] G. Jaworski, A. Francik, and K. Nowak, "TEm,1 coaxial modes generator for cold-testing of high power components and devices," *Bull. Pol. Acad. Sci. Tech. Sci.*, vol. 70, no. 2, p. e140467, 2022, doi: 10.24425/bpasts.2022.140467.

[2] L. Baranowski, "Effect of the mathematical model and integration step on the accuracy of the results of computation of artillery projectile flight parameters," *Bull. Pol. Acad. Sci. Tech. Sci.*, vol. 61, no. 2, pp. 475–484, 2013, doi: 10.2478/bpasts-2013-0047.

[3] M.C. Pak, K.I. Kim, H.C. Pak, and K.R. Hong, "Influence of geometric structure, convection, and eddy on sound propagation in acoustic metamaterials with turbulent flow," *Arch. Acoust.*, vol. 46, no. 4, pp. 637–647, 2021, doi: 10.24425/aoa.2021.139640.

[4] R.D. Graglia and G. Lombardi, "Machine precision evaluation of singular and nearly singular potential integrals by use of Gauss quadrature formulas for rational functions," *IEEE Trans. Antennas Propag.*, vol. 56, no. 4, pp. 981–998, Apr. 2008, doi: 10.1109/TAP.2008.919181.

[5] A. Herschlein, J.V. Hagen, and W. Wiesbeck, "Methods for the Evaluation of Regular, Weakly Singular and Strongly Singular Surface Reaction Integrals Arising in Method of Moments," *Appl. Comput. Electromagn. Soc. Newsl.*, vol. 17, no. 1, pp. 63–73, Mar. 2002.

[6] M.A. Khayat and D.R. Wilton, "Numerical evaluation of singular and near-singular potential integrals," *IEEE Trans. Antennas Propag.*, vol. 53, no. 10, pp. 3180–3190, Oct. 2005, doi: 10.1109/TAP.2005.856342.

[7] A.G. Polimeridis and J.R. Mosig, "Complete semi-analytical treatment of weakly singular integrals on planar triangles via the direct evaluation method," *Int. J. Numer. Methods Eng.*, vol. 83, no. 12, pp. 1625–1650, Sep. 2010, doi: 10.1002/NME.2877.

[8] D.J. Taylor, "Accurate and efficient numerical integration of weakly singular integrals in Galerkin EFIE solutions," *IEEE Trans. Antennas Propag.*, vol. 51, no. 7, pp. 1630–1637, Jul. 2003, doi: 10.1109/TAP.2003.813623.

[9] D.R. Wilton *et al.*, "Potential integrals for uniform and linear source distributions on polygonal and polyhedral domains," *IEEE Trans. Antennas Propag.*, vol. 32, no. 3, pp. 276–281, Mar. 1984, doi: 10.1109/TAP.1984.1143304.

[10] R.D. Graglia, "On the numerical integration of the linear shape functions times the 3-D Green's function or its gradient on a plane triangle," *IEEE Trans. Antennas Propag.*, vol. 41, no. 10, pp. 1448–1455, Oct.1993, doi: 10.1109/8.247786.

[11] S. Järvenpää, M. Taskinen, and P. Ylä-Oijala, "Singularity subtraction technique for high-order polynomial vector basis functions on planar triangles," *IEEE Trans. Antennas Propag.*, vol. 54, no. 1, pp. 42–49, Jan. 2006, doi: 10.1109/TAP.2005.861556.

[12] I. Hänninen, M. Taskinen, and J. Sarvas, "Singularity subtraction integral formulae for surface integral equations with RWG, rooftop and hybrid basis functions," *Prog. Electromagn. Res. PIER*, vol. 63, pp. 243–278, 2006. doi: 10.2528/PIER06051901.

[13] A.G. Polimeridis and T.V. Yioultsis, "On the direct evaluation of weakly singular integrals in Galerkin mixed potential integral equation formulations," *IEEE Trans. Antennas Propag.*, vol. 56, no. 9, pp. 3011–3019, Sep. 2008, doi: 10.1109/TAP.2008.928782.

[14] A.G. Polimeridis, F. Vipiana, J.R. Mosig, and D.R. Wilton, "DIRECTFN: Fully numerical algorithms for high precision computation of singular integrals in Galerkin SIE methods," *IEEE Trans. Antennas Propag.*, vol. 61, no. 6, pp. 3112–3122, Feb. 2013, doi: 10.1109/TAP.2013.2246854.

[15] S. Caorsi, D. Moreno, and F. Sidoti, "Theoretical and numerical treatment of surface integrals involving the free-space Green's function," *IEEE Trans. Antennas Propag.*, vol. 41, no. 9, pp. 1296–1301, Sep. 1993, doi: 10.1109/8.247757.

[16] M.S. Tong and W.C. Chew, "A novel approach for evaluating hypersingular and strongly singular surface integrals in electromagnetics," *IEEE Trans. Antennas Propag.*, vol. 58, no. 11, pp. 3593–3601, Nov. 2010, doi: 10.1109/TAP.2010.2071370.

[17] T.F. Eibert and V. Hansen, "On the calculation of potential integrals for linear source distributions on triangular domains," *IEEE Trans. Antennas Propag.*, vol. 43, no. 12, pp. 1499–1502, Dec. 1995, doi: 10.1109/8.475946.

[18] C. Balanis, *Advanced Engineering Electromagnetics*. New York, Chichester, Brisbane, Toronto, Singapore: Wiley, 1989, pp. 282–283.

[19] P.M. Słobodzian, *Electromagnetic Analysis of Shielde Microwave Structures. The Surface Integral Equation Approach*. Wrocław: Oficyna Wydawnicza Politechniki Wrocławskiej, 2007, pp. 135–136.

[20] A.A. Kucharski, *Analiza zagadnień promieniowania i rozpraszania fal elektromagnetycznych za pomocą równań całkowych*. Wrocław: Oficyna Wydawnicza Politechniki Wrocławskiej, 2012, pp. 39, 67.

[21] S.M. Rao, D.R. Wilton, and A.W. Glisson, "Electromagnetic scattering by surfaces of arbitrary shape," *IEEE Trans. Antennas Propag.*, vol. 30, no. 3, pp. 409–418, May 1982, doi: 10.1109/TAP.1982.1142818.

[22] R.F. Harrington, *Field computation by moment methods*. New York: Wiley, Sponsor: IEEE Antennas and Propagation Society, 1993, pp. 5–6.

[23] J.M. Jin, "The reference elements", in *The Finite Element Method in Electromagnetics*, 2nd ed., New York: Wiley, 2002, pp. 47–66.

[24] M. Abramowitz and I.A. Stegun, *Handbook of Mathematical Functions with Formulas, Graphs, and Mathematical Tables*. Washington: U.S. Government Printing Office, 1964.

[25] I.S. Gradshteyn and I.M. Ryzhik, *Table of contents for Table of Integrals, Series, and Products*. 6th ed., New York: Academic Press, 2000, doi: 10.1016/B978-0-12-294757-5.X5000-4.

[26] R.P. Brent and P.Zimmermann, "Integer arithmetic," in *Modern Computer Arithmetic*. Cambridge University Press, 2011, doi: 10.1017/CBO9780511921698.